Knowledge Discovery for Friction Stir Welding via Data-driven Approaches – Part 1: Correlation Analyses of Internal Process Variables and Weld Quality

Qian Zhang[a], Mahdi Mahfouf[a], George Panoutsos[a], Kathryn Beamish[b] and Ian Norris[b]

[a]Department of Automatic Control and Systems Engineering,
The University of Sheffield, Sheffield, S1 3JD, UK.
E-mail: {qian.zhang, m.mahfouf, g.panoutsos}@sheffield.ac.uk

[b]TWI Ltd, Great Abington, Cambridge, CB1 6AL, UK.
E-mails: {kathryn.beamish, ian.norris}@twi.co.uk

Abstract

For a comprehensive understanding towards Friction Stir Welding (FSW) which would lead to a unified approach that embodies materials other than aluminium, such as titanium and steel, it is crucial to identify the intricate correlations between the controllable process conditions, the observable internal process variables, and the characterisations of the post-weld materials. In Part I of this paper, multiple correlation analyses techniques have been developed to detect new and previously unknown correlations between the internal process variables and weld quality of aluminium alloy AA5083. Furthermore, a new exploitable weld quality indicator has, for the first time, been successfully extracted, which can provide an accurate and reliable indication of the 'as-welded' defects. All results relating to this work have been validated using real data obtained from a series of welding trials that utilised a new revolutionary sensory platform called ARTEMIS developed by TWI Ltd., the original inventors of the FSW process.

Keywords

1. Introduction

Friction Stir Welding (FSW) is a practical solid-state joining technique, which was invented at The Welding Institute (TWI), UK in 1991.[1] In a standard FSW process, a non-consumable rotating tool with a shoulder and a pin is inserted into the abutting edges of two rigidly clamped work pieces to be joined. The tool moves along the joint line with rotation while the shoulder makes firm contact with the top surface of the work pieces. During the process, material is softened by the heat generated from the friction between the tool and the work pieces, and is then transported from the front of the tool to the trailing edge where it is forged into a joint.[2] The FSW process involves severe plastic deformation, complex material flow and intricate thermo-mechanical processes, which finally result in a very complicated recrystallisation and development of texture in the weld.

In the FSW process, three essential groups of attributes can be identified, as illustrated in Fig. 1, i.e. process conditions, internal process variables and post-weld properties of the welds. The process conditions are the parameters used to control the welding process, such as tool rotational speed and welding speed (traverse speed). The internal process variables are those features that can be observed during the welding and can provide rich information about the undergoing process and the weld, such as the temperature profile of the tool, torque and forces of tool bearing. The post-weld properties include the weld quality, microstructural features, and mechanical properties of the welded material, which represent the status of the final product.

For the optimal process condition design, on-line monitoring and control of the friction stir welding, it is crucial to study the correlations among the process conditions, internal process variables and post-weld properties, and develop appropriate prediction models between them. For instance, in order to design a structurally sound, defect free and reliable weld via a 'reverse-engineering' fashion,[3,4] the accurate and robust prediction models for the post-weld properties considering process conditions as inputs should be firstly constructed, and then work as the 'core' in the subsequent optimal design. For on-line monitoring and control to prevent defect formation, the correlations between multiple, temporal internal process variables and the quality of weld produced should be well studied, and some reliable indices for the weld quality should be identified.

In this two-part paper, the above issues are investigated. In Part 1 of the paper, conventional statistical linear and non-linear correlation analyses, frequency analysis, as well as wavelet-based analysis techniques are employed to detect the correlation between the internal process variables and the weld quality. As a result, new exploitable indices are extracted to provide an effective indication of the 'as-welded' defects. As a second facet for this work (Part 2), a systematic data-driven modelling strategy will be developed to elicit intelligent models based on experimental data. Accurate and transparent predictive models for microstructures, mechanical properties, as well as internal process attributes will then be constructed.

The remainder of this paper is organised as follows. Section 2 introduces the basic details about the FSW experiments, including the material, the tool, the experimental settings, the monitoring system, and the post-weld tests for assessing the weld quality. Conventional statistical correlation analyses, frequency analysis, and wavelet-based analysis are then employed to reveal meaningful mappings between the internal process variables and the weld quality in Sections 3, 4, and 5, respectively. In Section 6, an optimisation paradigm is developed to generate a more accurate and practical weld quality indicator by integrating the previous analytical results together. Finally, concluding remarks are given in Section 7.

2. Experimental details

2.1 Material, tool and experimental settings

AA5083 is a non-heat treatable aluminium alloy, which has excellent corrosion resistance, good strength and formability.[5] In this work, 5.8 mm AA5083 plates were friction stir welded using a MX-Triflute[TM] tool.[6] All experimental trials are butt welds, which were made under position control with the tool at 0° tilt.

The Triflute[TM] concept has been proved to be a successful second generation FSW tool design, where three deep helical grooves are cut into the probe of the tool to encourage vertical movement of the weld metal. It can further feature a second thread with a shallower thread depth and pitch angle, which is referred to as MX (multi helix) design. The improvements in material flow introduced by the MX-Triflute[TM] tool design significantly increase the maximum achievable welding speed in aluminium

alloys.[7] In this work, the MX-Triflute[TM] tool was used in conjunction with a 25 mm diameter scroll shoulder.

For welding, two attributes are used to control the process: tool rotation speed (rpm) in clockwise or counter-clockwise direction and forward movement per revolution along the line of joint (or welding speed) (mm rev[-1]). The rotation of tool results in stirring and mixing of material around the rotating pin and the translation of tool moves the stirred material from the front to the back of the pin. Normally, a higher tool rotation speed generates higher temperature because of higher friction heating and results in more intense stirring and mixing of material.[8] In this work, an assessment was undertaken using a parameter test matrix consisting of five levels of tool rotation speed, 280,355,430, 505 and 580 rpm, and five levels of traverse feed rates, 0.6, 0.8, 1.0, 1.2, and 1.4 mm rev[-1].

2.2 On-line monitoring system

TWI has developed a novel FSW monitoring system for in-process collection of the internal data representing welding status. This system is an extensively instrumented rotating tool holder, which is named the Advanced Rotating Tool Environment Monitoring and Information System (Artemis). It can log data for a large amount of internal process variables in real time, such as tool temperature, shaft temperature, tool torque, traverse and axial compression forces of the tool, as shown in Fig. 2.

In addition, the Artemis unit can continuously characterise the tool lateral bending forces in multiple channels across the whole rotation of the tool. If these bending forces are displayed on a polar plot, then the instantaneous snapshot of the forces experienced by the tool will be accurately captured.[7] This provides a visualisation of the force profile during a complete 360° rotation of the FSW tool and is also called 'tool force footprint'. To study the tool bending forces for various positions when the tool is rotating, the rotation of the tool itself is evenly divided into 48 fixed angles according to the traverse direction. Fig. 3 shows an example of a polar plot, where the integers are data acquisition angle identifiers. Angle 37 is the traverse direction; Angles 38-48 and 1-12 lie on the retreating side of the weld; Angles 14-36 lie on the advancing side of the weld. In this work, all the above internal process variables were

recorded during several welding trials. They provide a whole new level of information for the FSW process and will be further studied in the following sections.

2.3 Assessment of weld quality

The common defects in friction stir welds are volumetric defects,[2] which are flow-related and formed due to inadequate or abnormal material stirring or mixing. For instance, with the tool rotating and traveling, the plastic deformed material around the tool pin firstly transfers layer by layer from the advancing side to the retreating side ahead the tool; hence a cavity will remain behind the advancing side of the tool. If the plastic material flowing back from the retreating side is not sufficient to fill the vacated region absolutely and instantaneously before cooling to still state, such defects will occur.[9]

To evaluate the quality of welds, three independent tests were conducted in this work, including a face bend test, a root bend test, and a cross-section inspection, to assess the impact of defects in the welds. For every single test, a sub-index is designed to express the degree of the weld quality. The values of such sub-indices are integers from 0 to 3, where 0 means free from identifiable flaws and 3 represents complete failure in bend tests or the presence of significant number of voids in the cross-section. By summing these sub-indices together, an overall weld quality index is obtained to represent the general situation for weld quality, whose value could be from 0 to 9 (0: excellent quality).

3. Statistical correlation analysis

In statistics, the Pearson's product-moment correlation coefficient 'r' is reflective of the linear correlation (or dependence) between two variables.[10] Its range is [-1, 1], where '1' or '-1' implies perfect linear correlation and '0' means no correlation. The correlation ratio 'η' is a more general dependency measure that can detect almost any functional dependency.[11] Its range is [0, 1], where '0' implies a small correlation, while '1' means a large correlation.

In this work, both of the dependency measures, correlation coefficient r and correlation ratio η, were employed to study the correlation between the internal process variables and the weld quality. The first experiment considered the

conventional internal process variables, including tool temperature, shaft temperature, tool torque, traverse force and axial compression force of the tool. As shown in Fig. 2, the Artemis unit has recorded the time-series data of these variables during the whole welding process. It is not practical to import all the temporal data in the correlation analysis. Consequently, only the most significant statistical features of them, including the maximum, minimum, mean and standard deviation in the steady state, were correlated with the post-weld quality. For the weld quality, both the sub-indices and the overall index were considered, which have been introduced in Section 2.3.

Tables 1 and 2 show the variables that are found to have the largest dependence with the weld quality in various aspects, according to the correlation coefficient and the correlation ratio, respectively. From the tables, it can be observed that the attributes relating to traverse force and shaft temperature are better correlated with the volumetric defects intentionally introduced. For more details, Fig. 4 shows the scatter plots relating to two of the discovered internal attributes, where the overall weld quality index is plotted against their own values. It can be seen that the maximum traverse force tends to be linearly dependent with the weld quality, while the mean of shaft temperature tends to non-linearly correlate with the weld quality. As mentioned in Section 2.3, the primary reason for the volumetric defect occurring lies in the insufficient or abnormal material flow during welding. As the tool traverse force could indicate the material flow, it is proper to identify the dependence between the traverse force and the weld quality. In addition, temperature is obviously another factor that highly relates to the formation of defects. A low temperature often relates to an inadequate heat input, which reduces the fluidity of the material and results in an insufficient material flow that cannot instantaneously fill the cavity remaining after the rotating FSW tool travels. However, a high temperature often relates to an excessive heat input, which increases the fluidity of the material and makes turbulent flow at the weld zone that increases the possibility of the formation of cavities.[12]

In the second experiment, the internal process variables relating to multiple tool bending forces on 48 angles were studied. In this analysis, the maximum, minimum, mean and standard deviation of their temporal data samples in the steady state were correlated with both of the sub-indices and the overall index of the weld quality. Tables 3 and 4 show the variables that are found to best correlate with the weld

quality according to the correlation coefficient and the correlation ratio, respectively. From these tables, it can be seen that, the weld quality has closer relationship with the tool bending forces locating in two certain areas, Angles 2-5 and Angles 21-31. As shown in Fig. 3, Angles 2-5 lie on the back of the retreating side of the weld, while Angle 21-31 lie on the edge of the advancing side. This suggests that these two independent areas may be relevant to void formation. Fig. 5 shows an example of the bending force variables for this experiment, where the overall weld quality index is plotted against its value. From the scatter plot, one can easily find that, with the mean of the tool bending force on Angle 2 increasing, the weld quality index clearly tends to increase.

4. Frequency analysis

The process of decomposing a function into simpler Fourier series and studying the series is often called Fourier analysis.[13] In signal processing, the Fourier transform often decomposes a function of time into simple sinusoids of different frequencies (frequency spectrum). Thus the Fourier analysis is also regarded as frequency analysis.

For FSW, it has been suggested that nonlinear oscillations of force signals are related to the dynamics of the plasticised material flow and may provide in-depth information about the mechanical process.[14] Therefore, by using the Fourier analysis, one may find some hidden clues in the frequency domain that can indicate the circumstance of the weld quality. In this work, the Fast Fourier Transform (FFT) algorithm[15] was employed to quickly evaluate the discrete version of the Fourier transform on computers.

For instance, Fig. 6 shows the discrete Fourier transform of one tool bending force for 3 different specimens. In this figure, the amplitude of the frequency spectrum has been normalised to the range from 0 to 1. The spike with the highest amplitude relates to the spindle frequency of the tool. It can be seen that, for the specimen without any defects, it has smaller amplitudes for high-frequency components, while the specimen with some defects includes a number of larger amplitudes in high-frequency region. Hence, the high-frequent amplitudes in the frequency spectra may correlate with the weld quality.

Based on the above findings, all of the internal process variables were further analysed. They were first transformed into the frequency domain. Their 100 highest amplitudes, which range from spindle frequency to sampling frequency, were then summed and tested in correlation with the overall weld quality using the correlation coefficient and correlation ratio measures. Table 5 shows the best internal variables found using this method and their values according to the dependency measures. It can be found that the defect formation seems to be directly related to the high-frequent oscillations of the tool bending forces in a particular region, i.e. Angles 32-36. Fig. 7 shows the scatter plot of the pair-wise data between the overall weld quality index and one of the acquired weld quality indicators. It can be clearly seen that, with the increase of the amplitude sum, the weld quality index increases.

5. Wavelet analysis

As introduced above, the Fourier transform can provide perfect frequency resolution, but no time information. In many situations, especially in real-life applications, one expects to localise a signal in both the time and frequency domains simultaneously. The wavelet transform is such a solution that might be deemed a form of time-frequency representation for temporal signals and so are related to different resolutions. Another advantage of the wavelet transform lies in the low computation complexity. For the fast Fourier transform algorithm,[15] the computation complexity O_f is $M\log_2 M$, where M is the length of a signal; while the wavelet transform only has a computation complexity $O_w = M$.[16] In addition, the wavelet transform is good at representing the functions with discontinuities and sharp peaks, and accurately deconstructing and reconstructing finite, non-periodic and non-stationary signals.

In general, a wavelet transform is the representation of a function by wavelets, which are scaled and translated copies of a finite-length or fast-decaying oscillating waveform. The wavelets are normally defined by a wavelet function $\psi(t)$ (mother wavelet) and a scaling function $\varphi(t)$ (father wavelet) in the time domain. The wavelet function can be viewed as a 'detail' function, which represents the variation information (high-frequency part) of the signal; while the scaling function is an 'approximation' function representing the average (low-frequency part) of the signal. In particular, after the wavelet transform, a signal $s(t)$ can be decomposed as the sum of two components:

$$s(t) = A\varphi(t) + \sum_{i=1}^{L} D_i \psi_i(t),$$

(1)

where A and D_i are the approximation and detail coefficients, respectively. L represents the level of wavelet transform. The wavelet transform is the process of obtaining the wavelet coefficients A and D_i based on certain types of wavelet and scaling functions. In this work, the simplest possible wavelet, Haar wavelet, was employed. It was initially proposed by Alfred Haar[17] and includes a certain sequence of rescaled 'square-shaped' functions. Its technical advantage is that it is good at analysing the signals with sudden transitions, such as monitoring of tool failure in machining.[18]

As discussed above, the nonlinear oscillations of the acquired internal process resultants generate from the FSW process nature and may contain in-depth information about the defect formation. In this work, the Haar wavelet was employed to study the internal process variables of the process. Hence, Fig. 8 gives the wavelet transform of one tool bending force for 3 different specimens. One phenomenon can be observed that, for the specimen with good weld quality, it has smaller detail coefficients D_1-D_3; while the specimen with bad weld quality includes a number of larger detail coefficients. Therefore, for these internal process variables, the sum of the detail coefficients in the wavelet analysis may suggest a high correlation with the weld quality.

The above finding was further examined using the statistical dependency measures. All internal process resultants were firstly wavelet transformed. The detail coefficients in different scale levels were then separately summed. Finally, these sums were tested in correlation with the overall weld quality. In this experiment, the wavelet transform carried out at a maximum level of 3. Table 6 provides 3 variables which were identified using this strategy and their values according to the dependency measures. Their dependency values are much higher than those obtained in the statistical correlation analysis in Section 3, but quite close to those acquired in the frequency analysis of Section 4. It should also be noted that the defect formation seems better related to the high-frequent oscillations in certain channels, such as Angles 35-36 and 45-46. Fig. 9 displays the specimens by plotting the overall weld

quality index against the sum of detail coefficients. It can be seen that, as the sum variable increases, the resulting weld quality index tends to increase.

6. Optimal design of weld quality indicator

Following the previous analyses, multiple factors have been identified to be functional to assess the FSW quality. In order to employ them in real-life applications, one may require an even more accurate and reliable indicator to be designed for on-line monitoring. A simple but practical way to achieve this is to design the indicator in a form of linear combination of the internal process variables as follows:

$$Ind(x) = \sum_i w_i V_i(x) + c, \tag{2}$$

where $V_i(x)$ are the variables identified in the previous analyses that can be well correlated with weld quality; w_i are weights and c is a constant, all of which need to be determined through an optimisation procedure; $Ind(x)$ is the desired weld quality indicator, whose value ranges from 0 to 1, where '0' represents the best quality while '1' means the worst quality.

To find the adequate weights w_i and constant c, the optimisation problem could be constructed as follows:

Optimisation objective: Maximise r_{Ind} towards 1, where r_{Ind} is the correlation coefficient value between $Ind(x)$ and the overall weld quality index according to the available experimental data x_k.

Constraints: $0 \leq Ind(x_k) \leq 1$ (3)

In this work, a salient nature-inspired optimisation algorithm, the Reduced Space Searching Algorithm (RSSA),[19,20] was employed. This algorithm was inspired by a simple human experience when searching for an 'optimal' solution to a 'real-life' problem, i.e. when humans search for a candidate solution given a certain objective, a large area tends to be scanned first; should one succeed in finding clues in relation to the predefined objective, then the search space is greatly reduced for a more detailed search. The most important difference between RSSA and other heuristic algorithms lies in the operation emphases within a search. Most of the optimisation algorithms concentrate on generating new solutions using various equations (derivative-related equations, PSO equations, etc.) or operators (mutation, recombination, etc.), while

RSSA concentrates on transforming the search space so as to find the 'optimal' sub-space and the generation of solutions within a sub-space does not constitute the real emphasis. Compared with some other evolutionary algorithms, RSSA performs as well as and sometimes better than those well-known optimisation algorithms.[19,20]

Assuming 5 internal process elements being chosen as $V_i(x)$, including the maximum of traverse force – $TF_{max}(x)$ (kN), the mean of shaft temperature – $ST_{mean}(x)$ (°C), the mean of the tool bending force on Angle 2 – $BF2_{mean}(x)$ (kN), the sum of 100 highest amplitudes in frequency spectrum of the tool bending force on Angle 34 – $SA_{BF34}(x)$ (kN), the sum of detail coefficients D_2 in Haar wavelet analysis of the tool bending force on Angle 46 – $SD2_{BF46}(x)$ (kN), then the following indicator can be generated after following optimisation:

$$Ind_1(x) = 0.027TF_{max}(x) + 0.016ST_{mean}(x) - 0.088BF2_{mean}(x) + 0.509SA_{BF34}(x) + 0.134SD2_{BF46}(x) - 1.913 \tag{4}$$

Table 7 shows its r value in comparison with other internal process variables and Fig. 10 exhibits its correlation with the weld quality intuitively. The merged indicator is obviously more accurate than a single internal process variable and hence more exploitable to serve the on-line quality assurance.

7. Conclusions

For on-line monitoring and control of the friction stir welding process, it is crucial to identify the correlations between the temporal internal process variables and the weld quality. In the paper, this problem has been studied using statistical linear and non-linear correlation analyses, Fourier frequency analysis, as well as wavelet analysis. As a result, some internal attributes have been detected to be well correlated with volumetric defect formation. Alternatively, an optimisation paradigm has been successfully developed to generate a more accurate and reliable weld quality indicator for on-line monitoring. In the next part of this work, a systematic data-driven modelling framework will be developed to construct accurate and interpretable predictive models for post-weld, microstructural and mechanical properties, as well as internal process features.

References:

[1] W. M. Thomas, E. D. Nicholas, J. C. Needham, M. G. Murch, P. Templesmith and C. J. Dawes: G.B. Patent Application No. 9125978.8, December 1991.

[2] R. Nandan, T. DebRoy and H. K. D. H. Bhadeshia: 'Recent advances in friction stir welding - process, weldment structure and properties', *Progress in Materials Science*, 2008, **53**, 980–1023.

[3] Q. Zhang, M. Mahfouf, J. R. Yates, C. Pinna, G. Panoutsos, S. Boumaiza, R. J. Greene and L. de Leon: 'Modeling and Optimal Design of Machining-Induced Residual Stresses in Aluminium Alloys Using a Fast Hierarchical Multiobjective Optimization Algorithm', *Materials and Manufacturing Processes*, 2011, **26** (3), 508-520.

[4] Q. Zhang and M. Mahfouf: 'A Hierarchical Mamdani-Type Fuzzy Modelling Approach with New Training Data Selection and Multi-Objective Optimisation Mechanisms: a Special Application for the Prediction of Mechanical Properties of Alloy Steels', *Applied Soft Computing*, 2011, **11** (2), 2419-2443.

[5] E. A. El-Danaf, M. M. El-Rayes and M. S. Soliman: 'Friction stir processing: An effective technique to refine grain structure and enhance ductility', *Materials and Design*, 2010, **31**, 1231–1236.

[6] W. M. Thomas and M. F. Gittos: 'Development of friction stir tools for the welding of thick (25mm) aluminium alloys', TWI Members Report 694/1999, UK, December 1999.

[7] K. A. Beamish and M. J. Russell: 'Relationship between the features on an FSW tool and weld microstructure', Proceedings of the 8th International Symposium on Friction Stir Welding, Timmendorfer Strand, Germany, 2010.

[8] R. S. Mishra and Z. Y. Ma: 'Friction stir welding and processing', *Materials Science and Engineering R: Reports*, 2005, **50** (1-2), 1–78.

[9] B. Li, Y. Shen and W. Hu: 'The study on defects in aluminum 2219-T6 thick butt friction stir welds with the application of multiple non-destructive testing methods', *Materials and Design*, 2011, **32**, 2073–2084.

[10] J. L. Rodgers and W. A. Nicewander: 'Thirteen ways to look at the correlation coefficient', *The American Statistician*, 1988, **42** (1), 59–66.

[11] J. F. Kenney and E. S. Keeping: 'Mathematics of statistics', 2nd edn; 1951, Van Nostrand, NJ, Princeton.

[12] A. M. Gaafer, T. S. Mahmoud and E. H. Mansour: 'Microstructural and mechanical characteristics of AA7020-O Al plates joined by friction stir welding', *Materials Science and Engineering A*, 2010, **527**, 7424–7429.

[13] G. Kaiser: 'A Friendly Guide to Wavelets', 1994, Boston, Birkhäuser.

[14] E. Boldsaikhana, E. M. Corwinb, A. M. Logarb and W. J. Arbegast: 'The use of neural network and discrete Fourier transform for real-time evaluation of friction stir welding', *Applied Soft Computing*, 2011, **11**, 4839–4846.

[15] J. W. Cooley and J. W. Tukey: 'An algorithm for the machine calculation of complex Fourier series', *Math. Comput.*, 1965, **19** (90), 297–301.

[16] S. W. Smith: 'The scientist and engineer's guide to digital signal processing', 1997, California Technical Publishing

[17] A. Haar: 'Zur Theorie der orthogonalen Funktionensysteme', *Mathematische Annalen*, 1910, **69** (3), 331–371.

[18] B. Lee and Y. S. Tarng: 'Application of the discrete wavelet transform to the monitoring of tool failure in end milling using the spindle motor current', *International Journal of Advanced Manufacturing Technology*, 1999, **15** (4), 238–243.

[19] Q. Zhang and M. Mahfouf: 'A new Reduced Space Searching Algorithm (RSSA) and its application in optimal design of alloy steels', Proceedings of the 2007 IEEE Congress on Evolutionary Computation, Singapore, 2007, 1815-1822.

[20] Q. Zhang and M. Mahfouf: 'A nature-inspired multi-objective optimisation strategy based on a new reduced space searching algorithm for the design of alloy steels', *Engineering Applications of Artificial Intelligence*, 2010, **23** (5), 660–675.

Figures
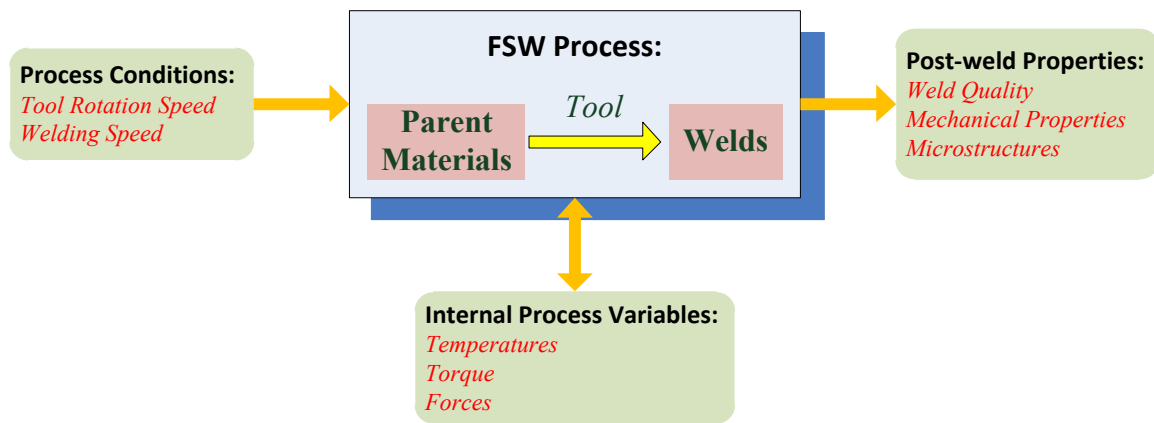
Fig. 1. The essential properties involved in FSW.
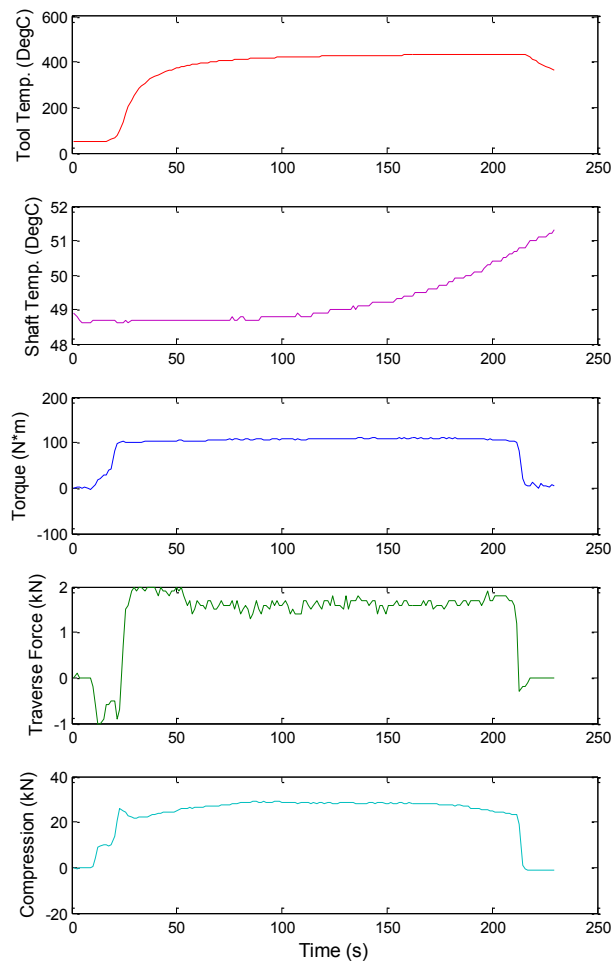
Fig. 2. An example of internal process variables observed by the 'Artemis' system: a butt weld of 5.8 mm AA5083 plates using a MX-TrifluteTM tool, with a tool rotation speed 505 rpm and a traverse feed rate 0.6 mm/rev.
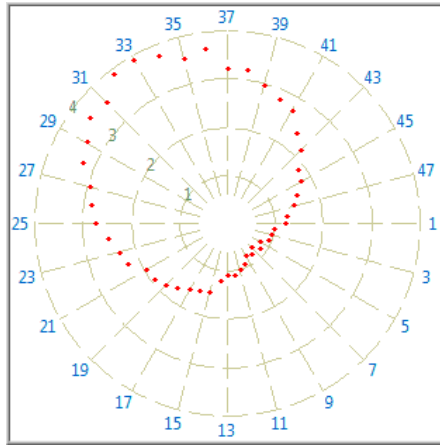
Fig. 3. An example of tool force footprint in the steady state of the welding: one inner cycle represents 1kN each and Angle 37 represents the traverse direction.

(a)   (b)

Fig. 4. The scatter plots of the FSW specimens: (a) the overall weld quality index vs. the maximum of traverse force, and (b) the overall weld quality index vs. the mean of shaft temperature.

Fig. 5. The scatter plot of the FSW specimens: the overall weld quality index vs. the mean of the tool bending force on Angle 2.
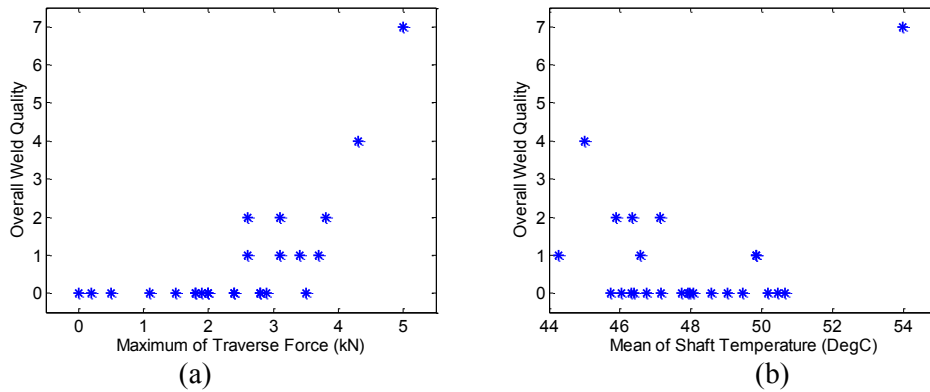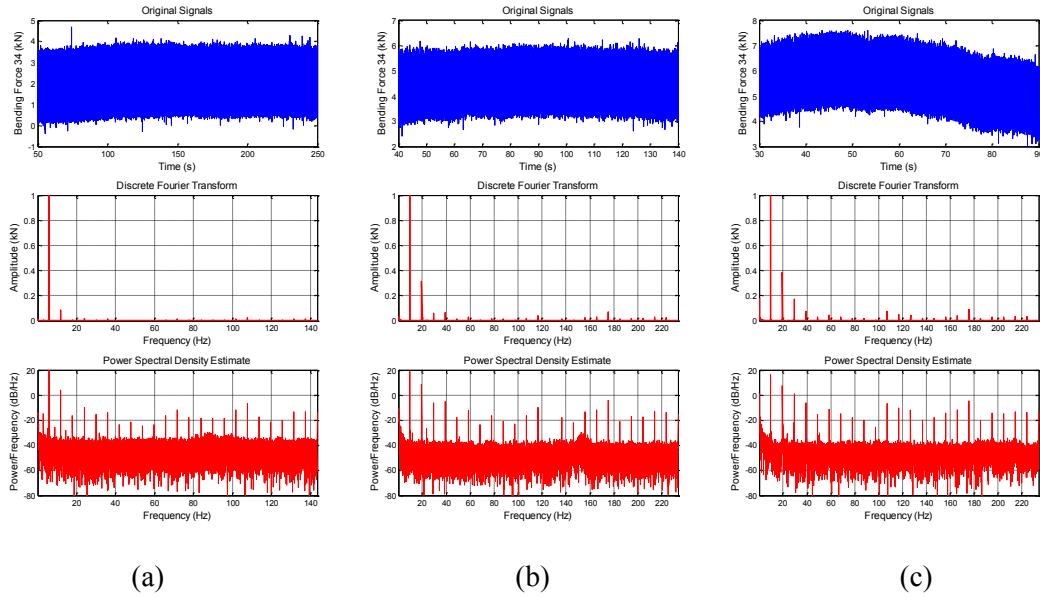
Fig. 6. Fourier transform of the tool bending force on Angle 34 for: (a) a specimen with good weld quality, (b) a specimen with medium weld quality, and (c) a specimen with bad weld quality.
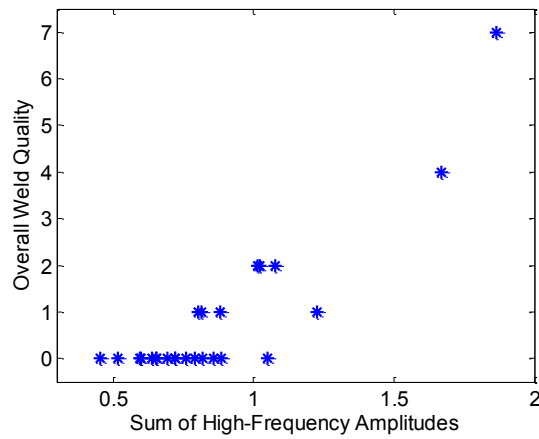
Fig. 7. The scatter plot of the FSW specimens: the overall weld quality index vs. the sum of 100 highest amplitudes in the frequency spectrum of the tool bending force on Angle 34.

(a)   (b)   (c)
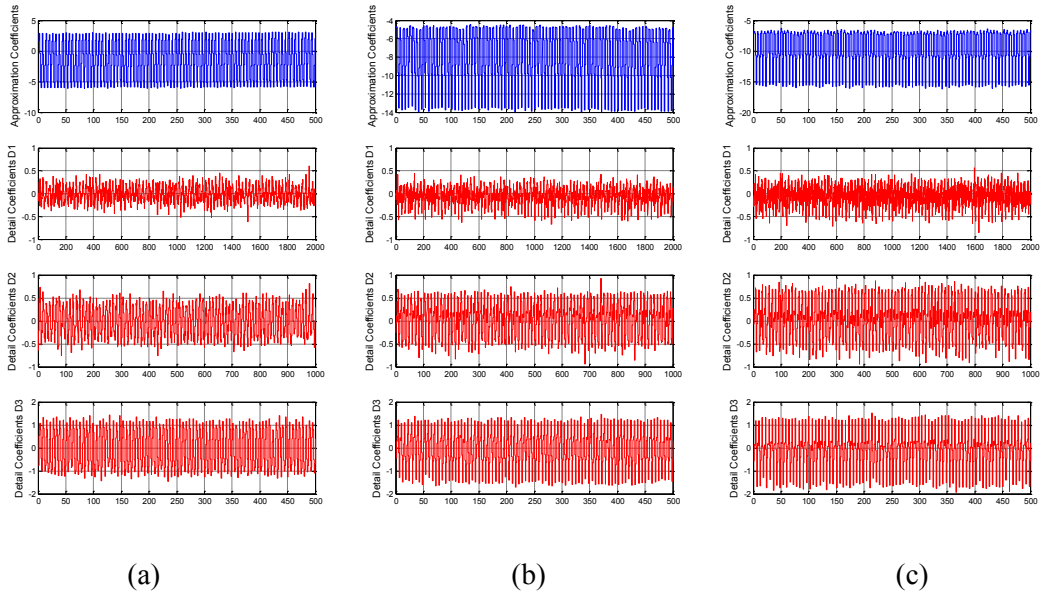
Fig. 8. Haar wavelet transform of the tool bending force on Angle 46 for: (a) a specimen with good weld quality, (b) a specimen with medium weld quality, and (c) a specimen with bad weld quality.
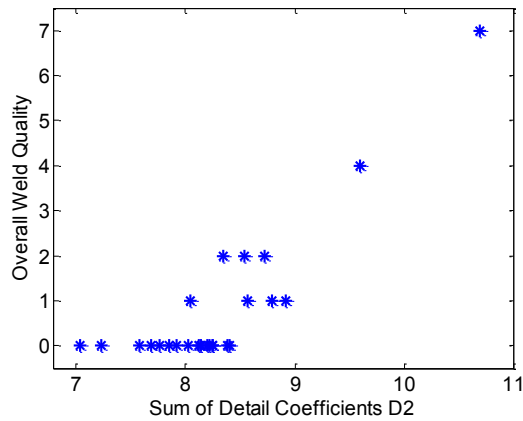
Fig. 9. The scatter plot of the FSW specimens: the overall weld quality index vs. the sum of detail coefficients D_2 in Haar wavelet analysis of the tool bending force on Angle 46.
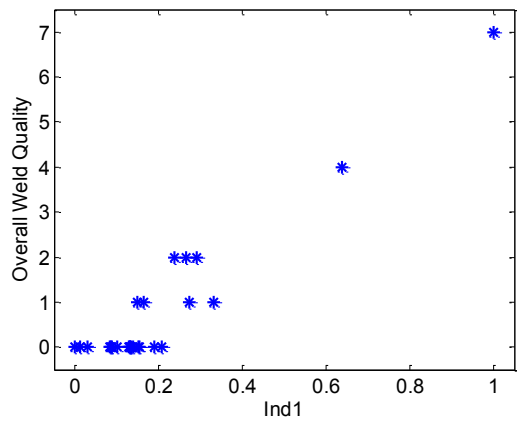
Fig. 10. The scatter plot of the FSW specimens: the overall weld quality index vs. Ind_1.

Tables

Table 1. The internal process variables that were detected to be best correlated with the FSW quality by correlation coefficient r.

Linear Correlation	1st best correlated variable (r value)	2nd best correlated variable (r value)	3rd best correlated variable (r value)
Sub-index of face bend test	Min of torque (-0.5571)	Mean of torque (-0.5306)	Max of torque (-0.5265)
Sub-index of root bend test	Mean of shaft temperature (0.6204)	Min of shaft temperature (0.5822)	Max of shaft temperature (0.4265)
Sub-index of cross-section inspection	Min of traverse force (0.6796)	Mean of traverse force (0.6796)	Max of traverse force (0.6547)
Overall weld quality index	Min of traverse force (0.7055)	Mean of traverse force (0.6930)	Max of traverse force (0.6843)

Table 2. The internal process variables that were detected to be best correlated with the FSW quality by correlation ratio η.

Non-linear Correlation	1st best correlated variable (η value)	2nd best correlated variable (η value)	3rd best correlated variable (η value)
Sub-index of face bend test	Max of compression (0.6598)	Min of torque (0.6258)	Max of torque (0.6136)
Sub-index of root bend test	Mean of shaft temperature (0.9544)	Min of shaft temperature (0.9531)	Max of traverse force (0.6497)
Sub-index of cross-section inspection	Mean of traverse force (0.8944)	Min of traverse force (0.8882)	Max of traverse force (0.8790)
Overall weld quality index	Max of traverse force (0.9055)	Mean of traverse force (0.8860)	Min of traverse force (0.8805)

Table 3. The tool bending forces that were detected to be best correlated with the FSW quality by correlation coefficient r.

Linear Correlation	1st best correlated variable (r value)	2nd best correlated variable (r value)	3rd best correlated variable (r value)
Sub-index of face bend test	Min of the bending force on Angle 45 (0.4745)	Min of the bending force in Angle 43 (0.4658)	Min of the bending force on Angle 46 (0.4644)
Sub-index of root bend test	Std of the bending force on Angle 22 (0.5664)	Std of the bending force on Angle 23 (0.5305)	Max of the bending force on Angle 3 (0.5146)
Sub-index of cross-section inspection	Mean of the bending force on Angle 5 (0.7517)	Std of the bending force on Angle 21 (0.7516)	Max of the bending force on Angle 5 (0.7515)
Overall weld quality index	Mean the bending force on Angle 4 (0.7737)	Mean of the bending force on Angle 3 (0.7728)	Min of the bending force on Angle 4 (0.7701)

Table 4. The tool bending forces that were detected to be best correlated with the FSW quality by correlation ratio η.

Non-linear Correlation	1st best correlated variable (η value)	2nd best correlated variable (η value)	3rd best correlated variable (η value)
Sub-index of face bend test	Min of the bending force on Angle 5 (0.5404)	Min of the bending force on Angle 6 (0.5404)	Min of the bending force on Angle 4 (0.5335)
Sub-index of root bend test	Std of the bending force on Angle 24 (0.9544)	Std of the bending force on Angle 22 (0.9531)	Std of the bending force on Angle 25 (0.9531)
Sub-index of cross-section inspection	Min of the bending force on Angle 27 (0.9487)	Mean of the bending force on Angle 28 (0.9462)	Mean of the bending force on Angle 31 (0.9462)
Overall weld quality index	Mean of the bending force on Angle 2 (0.9035)	Max of the bending force on Angle 2 (0.9035)	Min of the bending force on Angle 2 (0.8997)

Table 5. The internal process variables that were detected to be best correlated with the overall FSW quality using the frequency analysis method.

Overall weld quality index	1st best correlated variable	2nd best correlated variable	3rd best correlated variable
Linear Correlation (r value)	Bending force on Angle 35 (0.8953)	Bending force on Angle 34 (0.8926)	Bending force on Angle 36 (0.8903)
Non-linear Correlation (η value)	Bending force on Angle 34 (0.9551)	Bending force on Angle 33 (0.9340)	Bending force on Angle 32 (0.9244)

Table 6. The internal process variables that were detected to be best correlated with the overall FSW quality using the Haar wavelet analysis method.

Overall weld quality index	1st best correlated variable	2nd best correlated variable	3rd best correlated variable
Linear Correlation (r value)	Sum of D_2 of the bending force on Angle 46 (0.8640)	Sum of D_3 of the bending force on Angle 35 (0.8465)	Sum of D_2 of the bending force on Angle 45 (0.8448)
Non-linear Correlation (η value)	Sum of D_2 of the bending force on Angle 46 (0.9545)	Sum of D_2 of the bending force on Angle 29 (0.9256)	Sum of D_3 of the bending force on Angle 36 (0.9188)

Table 7. The comparison between Ind_1 and other internal process variables according to correlation coefficient r.

	r value between one and overall weld quality
Maximum of traverse force	0.6843
Mean of shaft temperature	0.2519
Mean of the tool bending force on Angle 2	0.7575
Sum of the highest frequency spikes of the tool bending force on Angle 34	0.8926
Sum of D_2 in wavelet analysis of the tool bending force on Angle 46	0.8640
Ind_1	0.9506